Interaction of the Shiga-like Toxin Type 1 B-Subunit with Its Carbohydrate Receptor†

Phaedria M. St. Hilaire,‡ Mary K. Boyd,§ and Eric J. Toone*,‡

Department of Chemistry, Duke University, Durham, North Carolina 27708-0346, and Department of Chemistry, Loyola University of Chicago, Chicago, Illinois 60626

Received August 24, 1994⊗

ABSTRACT: A study of the binding of the Shiga-like toxin 1 (SLT-1) to the P^k trisaccharide [methyl 4-*O*-(4-*O*-α-D-galactopyranosyl)-4-*O*-β-D-galactopyranosyl-β-D-glucopyranoside] and its constituent dissaccharides was carried out. The trisaccharide represents the carbohydrate recognition domain of the neutral glycolipid receptor of the SLT-1, globotriosylceramide ($GbOse_3$). The binding constant for soluble trisaccharide to the soluble pentameric B-subunit is weak, with a K_a of $(0.5-1) \times 10^3$ M^{-1} for B-subunit monomer. Scatchard analysis of the binding data indicates five identical non-interacting carbohydrate binding sites per B-subunit pentamer and no cooperativity in binding. Despite weak binding ($\Delta G = -3.6$ kcal mol^{-1}), the enthalpy of binding ($\Delta H = -12$ kcal mol^{-1}) and the change in molar heat capacity accompanying binding ($\Delta C_p = -40$ eu) are comparable to other protein−carbohydrate interactions. Dynamic light scattering studies indicate that carbohydrate binding induces protein aggregation. At carbohydrate concentrations where >90% of B-subunit monomers are bound, the far-UV CD spectra were unchanged, whereas a change in the near-UV CD, maximal near 270 nm, titrated to give an apparent binding constant in good agreement with that obtained by isothermal microcalorimetry. Steady-state fluorescence and fluorescence lifetime measurements indicated that the environments of the central tryptophans are perturbed during saccharide binding, and the changes correlate with the extent of protein aggregation. On the basis of the thermodynamics of binding, optical spectroscopy, and binding-induced aggregation, we propose a model of SLT-1−membrane interaction that relies on protein−carbohydrate interaction for specificity and protein−lipid interaction for tight binding.

Diarrheal diseases claim millions of lives annually in the developing world (Stoll et al., 1982; Rhode, 1984). The pathologies of the most severe enterotoxic bacteria can be traced to a group of related two-component protein toxins, including the cholera toxin (cholera), the Shiga and Shiga-like toxins (shigellosis), and the *Escherichia coli* heat-labile toxins (traveler's diarrhea). While diarrheal diseases are not currently a major health concern in the Western world, there are indications that they are fast becoming a significant threat to human health worldwide (IOM Report, 1992; CDC Report, 1993). The genes encoding many bacterial two-component toxins, including the cholera and Shiga toxins, are either phage or plasmid encoded (Strockbine et al., 1986); both toxins have now been identified in species other than *Vibrio* and *Shigella*, respectively, most significant in *E. coli*. Recent outbreaks of the Shiga toxin-producing *E. coli* O157:H7 underscore the developing threat associated with the rapid emergence of toxin-producing bacterial strains (Griffin & Tauxe, 1991; Lee et al., 1991; CDC Report, 1993). The development and spread of such organisms, coupled with the surprising appearance of organisms resistant to conventional antimicrobial therapies, provide strong motivation for the development of novel therapeutic agents for the clinical management of bacterial toxin poisoning.

Bacterial enterotoxins are structurally related to a larger group of proteins that includes the botulinum, pertussis, and diphtheria toxins (Keusch et al., 1986). In each case, the active holotoxin consists of a single enzymatically active A-subunit and multiple copies of a binding or B-subunit (Keusch et al., 1986). The binding subunits are lectins that recognize and adhere to host cell-surface glycoconjugates. Following binding, the toxins are endocytosed from either clathrin-coated or uncoated pits, and the A-subunit is transported to the cytosol. Because the binding subunits are lectins, a potential therapy for enterotoxin poisoning would utilize small molecule carbohydrate mimics to prevent toxin adhesion. We have begun an investigation of the feasibility of this approach for the Shiga-like toxin 1, or SLT-1.[1]

The SLT-1, expressed by several strains of *E. coli*, is virtually identical both in structure and mechanism of action to the toxin expressed by *Shigella dysenteriae 1*, the causative agent of shigellosis (Strockbine et al., 1988). The SLT-1 holotoxin comprises a single 32 kDa A-subunit and five copies of a B-subunit (Seidah et al., 1986; Strockbine et al., 1988). With a molecular mass of 7.7 kDa, the SLT-1 B-subunit is among the smallest known lectins. Crystal structures of both the B-subunit pentamer and the holotoxin have been solved and deposited (Stein et al., 1992; Fraser et al., 1994). The B-subunits are arranged as a symmetrical pentamer, with the A-subunit located above the center of one face. Following binding to a glycolipid receptor, the

† P.M.S.H. was a 1990−1993 CIIT Toxicology Training Grant Fellow.

‡ Duke University.

§ Loyola University of Chicago.

⊗ Abstract published in *Advance ACS Abstracts,* November 1, 1994.

[1] Abbreviations: $GbOse_3$, globotriosylceramide; P^k trisaccharide, methyl 4-*O*-(4-*O*-α-D-galactopyranosyl)-4-*O*-β-D-galactopyranosyl-β-D-glucopyranoside; SLT-1, Shiga-like toxin 1; MOPS, 3-morpholinopropanesulfonic acid; ELAM, endothelial leukocyte adhesion molecule; PBS, phosphate-buffered saline; eu, entropy units (calories $mole^{-1}$ $degree^{-1}$).

0006-2960/94/0433-14452$04.50/0

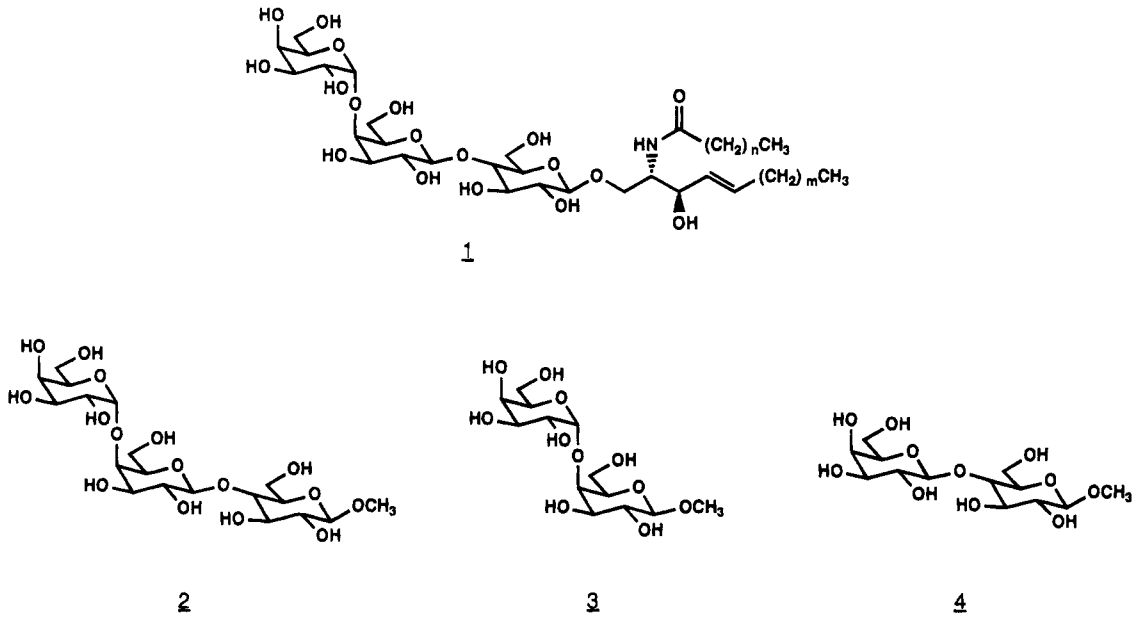

FIGURE 1: Globotriosylceramide ($GbOse_3$, **1**), the P^k trisaccharide (**2**), β-methyl galabioside (**3**), and β-methyl lactoside (**4**).

toxin is endocytosed from chalthrin-coated pits and transferred first to the trans Golgi network and subsequently to the endoplasmic reticulum and nuclear envelope (Sandvig et al., 1989, 1991, 1992). While it appears that transfer of the toxin to the Golgi apparatus is essential for intoxication by the Shiga toxin (Sandvig et al., 1991), the mechanism of entry of the A-subunit from the endosome to the cytosol, and particularly the role of the B-subunit in the process, remains unclear. In the cytosol the A-subunit acts as an *N*-glycosidase, inhibiting protein biosynthesis at the ribosomal level (Brown et al., 1980; Reisbig et al., 1981). In the absence of the A-subunit, the B-subunit forms pentamers that are functionally identical to those in holotoxin in binding assays (Donohue-Rolfe et al., 1989).

Shiga/Shiga-like toxins produce a unique hemorrhagic colitis that, in roughly 10% of cases, proceeds to hemolytic uremic syndrome (Griffin et al., 1988). The latter condition is frequently fatal, and only palliative treatments currently are available. There is evidence that both antibiotic and antimotility therapies exacerbate the disease (Cimolai et al., 1990; Walterspiel et al., 1992). The *in vivo* receptor of the Shiga and Shiga-like toxins is the trisaccharide portion of the neutral glycolipid, globotriosylceramide [$GbOse_3$, αGal(1→4)βGal(1→4)βGlc(1→1)-ceramide (**1**)] (Lindberg et al., 1987), although some solid-phase assays have identified other oligosaccharides containing a terminal αGal(1→4)Gal linkage as SLT-1 ligands (Lindberg et al., 1986; Lingwood et al., 1987; Brown et al., 1991). The renal toxicity of the toxins is thought to reflect the high concentration of $GbOse_3$ in kidney tissue (Boyd & Lingwood, 1989), and the Shiga and Shiga-like toxins are sometimes referred to as verotoxins, reflective of their toxicity toward Vero (Green monkey kidney) cells.

As a preface to the preparation of potential inhibitors of Shiga toxin binding, we have investigated the thermodynamics of binding of SLT-1 to the carbohydrate domain of its native receptor αGal(1→4)βGal(1→4)-βGlcOMe (**2**, the P^k trisaccharide) and the constituent disaccharides αGal(1→4)βGalOMe (**3**, β-methyl galabioside) and βGal(1→4)βGlcOMe (**4**, β-methyl lactoside) using isothermal titration microcalorimetry. We report here the first detailed thermodynamic study of SLT-1 oligosaccharide interaction. Because our studies identified a binding-induced aggregation, we carried out both CD and fluorescence spectroscopic investigations of free and saccharide-bound SLT B-subunit to evaluate saccharide-induced structural perturbations in the B-subunit that lead to aggregation.

MATERIALS AND METHODS.

General. All buffers and salts were purchased from Sigma Chemical Co. and used without further purification. Water for all experiments was purified using a Waters Millipure system. Carbohydrate concentrations were measured using the phenol/sulfuric acid char method of Dubois (Dubois et al., 1956), and protein concentrations were measured by the method of Edelhoch (Edelhoch, 1967). Throughout, the B-subunit concentrations given are of monomer unless specified otherwise.

Synthesis of Carbohydrates. Methyl 4-*O*-(β-D-galactopyranosyl)-β-D-glucopyranoside (**4**), methyl 4-*O*-(α-D-galactopyranosyl)-β-D-galactopyranoside (**3**), and methyl 4-*O*-(4-*O*-α-D-galactopyranosyl)-4-*O*-β-D-galactopyranosyl-β-D-glucopyranoside (**2**) were synthesized by modifications of literature methods (Cox et al., 1978; Garregg & Oscarson, 1985); details of the syntheses are contained in the supplementary material. In all cases oligosaccharides were >95% pure by NMR.

SLT-1 B-Subunit. Native and F30A mutant SLT-1 B-subunits were purified from high-expression clones JB122 and 30B11R obtained from Professor J. Brunton, The University of Toronto/The Toronto Hospital. The B-subunit was purified using a combination of ion exchange chromatography and chromatofocusing. Details of both clone construction and protein purification have been reported elsewhere (Ramotar et al., 1990).

Calorimetry. All titrations were performed on a Microcal Omega titration microcalorimeter thermostated with an external bath to 5 °C below the operating temperature. To a solution of protein in a total cell volume of 1.3678 mL was added carbohydrate in aliquots of 2−8 μL. The additions were performed on a regular time schedule, with 2−3 min intervals between injections. The injections were controlled by a 386-based microcomputer. Experimental

details for individual runs are provided in the figure legends. The instrument design and characteristics have been published elsewhere (Wiseman et al., 1989).

The details of data reduction are recorded elsewhere (Bevington, 1969; Wiseman et al., 1989). Briefly, in a calorimetric titration, the heat evolved during each injection, q_n, is related to the enthalpy of binding, ΔH, by the expression

$$q_n = \Delta H([\mathrm{LP}]_n - [\mathrm{LP}]_{(n-1)}) \quad (1)$$

where [LP] represents the ligand−protein complex concentration. The heat generated at each injection is related to the binding constant, K, by the expression

$$1/V_o(dq/d[L]_{tot}) = \Delta H\left[{}^1/_2 + \frac{1 - (1+r)/2 - [\mathrm{L}]_r/2}{([\mathrm{L}]_r^2 - 2[\mathrm{L}]_r(1-r) + (1+r)^2)^{1/2}}\right] \quad (2)$$

where $1/r = [\mathrm{P}]_{tot}K$ and $[\mathrm{L}]_r = [\mathrm{L}]_{tot}/[\mathrm{P}]_{tot}$. V_o represents the cell volume, while $[\mathrm{P}]_{tot}$ and $[\mathrm{L}]_{tot}$ represent the total protein and ligand concentrations, respectively. From the integrated enthalpies following each addition of ligand, a binding constant, K, an enthalpy of binding, ΔH, and a stoichiometry of binding, n, are extracted through a nonlinear least-squares fit of the data to expression 2. Non-negligible heats of dilution were subtracted prior to data reduction.

Heat capacity changes were determined by evaluating ΔH as a function of temperature over the range 10−40 °C. The change in heat capacity accompanying binding, ΔC_p, is rigorously defined as $(\partial H/\partial T)_p$. Over short temperature ranges, ΔC_p is predicted to be linear and can be approximated by $(\Delta H_1 - \Delta H_2)/(T_1 - T_2)$.

Scatchard Plots. The concentration of bound ligand on the ith injection, $[\mathrm{LP}]_i$, can be calculated from the measured enthalpy, q_i, as follows:

$$[\mathrm{LP}]_i = \frac{\text{moles of saccharide added}}{\text{cell volume}} q_i/q_{max} \quad (3)$$

where q_i is the evolved heat on the ith injection and q_{max} is the enthalpy that would result from the complete binding of added ligand. After the ith injection, the total bound ligand [LP] is given by

$$[\mathrm{LP}] = [\mathrm{LP}]_i + 0.9949[\mathrm{LP}]_{i-1} \quad (4)$$

where the factor 0.9949 corrects for the ~0.5% dilution of cell contents upon each injection. Then v is given by

$$v = [\mathrm{LP}]/[\mathrm{P}]_{tot} \quad (5)$$

where $[\mathrm{P}]_{tot}$ is the B-subunit pentamer concentration, corrected for dilution on each injection. The free ligand concentration after the ith injection, [L], is given by $[\mathrm{L}]_{tot} - [\mathrm{LP}]$. Scatchard plots were created by plotting $v/[\mathrm{L}]$ vs. v.

Dynamic Light Scattering. Spectra were recorded at 25 °C on a Malvern 4700 V4 instrument using a 4 W argon laser at an angle of 90° to the detector. To a solution of the B-subunit (0.200 mM) in PBS buffer (pH 7.38) was added a solution of the P^k trisaccharide (70 mM) in PBS (pH 7.38) in 5 μL aliquots. After each addition of saccharide, three measurements were made over 15 min. No increase in particle size was observed for any carbohydrate concentration beyond that time.

Circular Dichroism Studies. CD spectra of native and mutant B-subunits were collected at 30 °C on an AVIV 62DS spectrometer. Far-UV spectra were recorded in a 10 mm cell (2.5 mL) between 199 and 280 nm. After each addition of saccharide, four scans, 1 min apart, were collected and averaged to give the final spectrum. Near-UV spectra were recorded in a similar manner between 250 and 325 nm. Blank runs of carbohydrate in buffer were recorded and subtracted from those of protein and carbohydrate before final analysis of the difference spectra. Details of individual runs are reported in the figure legends.

Fluorescence Spectroscopy. The excitation/emission matrix of native B-subunit was recorded at 25 °C on an SLM Aminco 48000S spectrofluorometer. Steady-state fluorescence spectra and lifetimes of native and mutant B-subunits were measured at 25 °C on a PTI LS-100 spectrofluorometer. Excitation was at 295 nm, and emission intensity and fluorescence lifetimes were recorded before and after the addition of carbohydrate. Details of individual runs are reported in the figure legends.

RESULTS AND DISCUSSION

Calorimetry. Raw and integrated data for SLT-1 B-subunit P^k trisaccharide binding are shown in Figure 2. Data reduction of SLT-1 B-subunit association with the P^k trisaccharide gave binding constants of $(0.5-1) \times 10^3$ M^{-1} per monomer. Protein−carbohydrate binding constants are typically in the range of 10^3-10^6 M^{-1}: even by this standard the SLT-1−P^k trisaccharide binding constant is remarkably weak. Because the lectin is pentameric, a binding constant of ~10^3 M^{-1} is low but not inconsistent with binding constants of 10^9 M^{-1} that have been reported for the binding of holotoxin to rabbit jejunal microvillus membranes (Fuchs et al., 1986). Plots of integrated evolved heat vs ligand concentration show no sigmoidal deviation from the expected shape, suggesting an absence of cooperative binding (Figure 3). In contrast, plots of integrated evolved heat vs ligand concentration for the interaction of the closely related cholera toxin with the carbohydrate portion of G_{M1} show a sigmoidal deviation; the curvature was interpreted in terms of positive cooperativity (Schön & Freire, 1989).

Integrated data for the binding of β-methyl galabioside, β-methyl lactoside, and the P^k trisaccharide to the B-subunit are shown in Figure 4. Although the binding is too weak to accurately determine binding constants, it is clear that β-methyl galabioside binds to the B-subunit, while any interaction of β-methyl lactoside with the B-subunit is too weak to detect. This is in keeping with previous observations that the B-subunit binds to glycolipids containing a terminal αGal(1→4)Gal linkage, but not to lactose-containing glycoconjugates (Lindberg et al., 1986; Lingwood et al., 1987; Brown et al., 1991). The interaction of the B-subunit with the monosaccharide β-methylgalactose and α-methylmannose showed no exothermicities upon the addition of saccharide (data not shown).

Despite a low interaction energy ($\Delta G = -3.6$ kcal mol^{-1}), the binding of the SLT-1 B-subunit to the P^k trisaccharide is strongly exothermic ($\Delta H = -12$ kcal mol^{-1}) and opposed by a large unfavorable entropic component. The enthalpy and entropy of the interaction are thus comparable to those

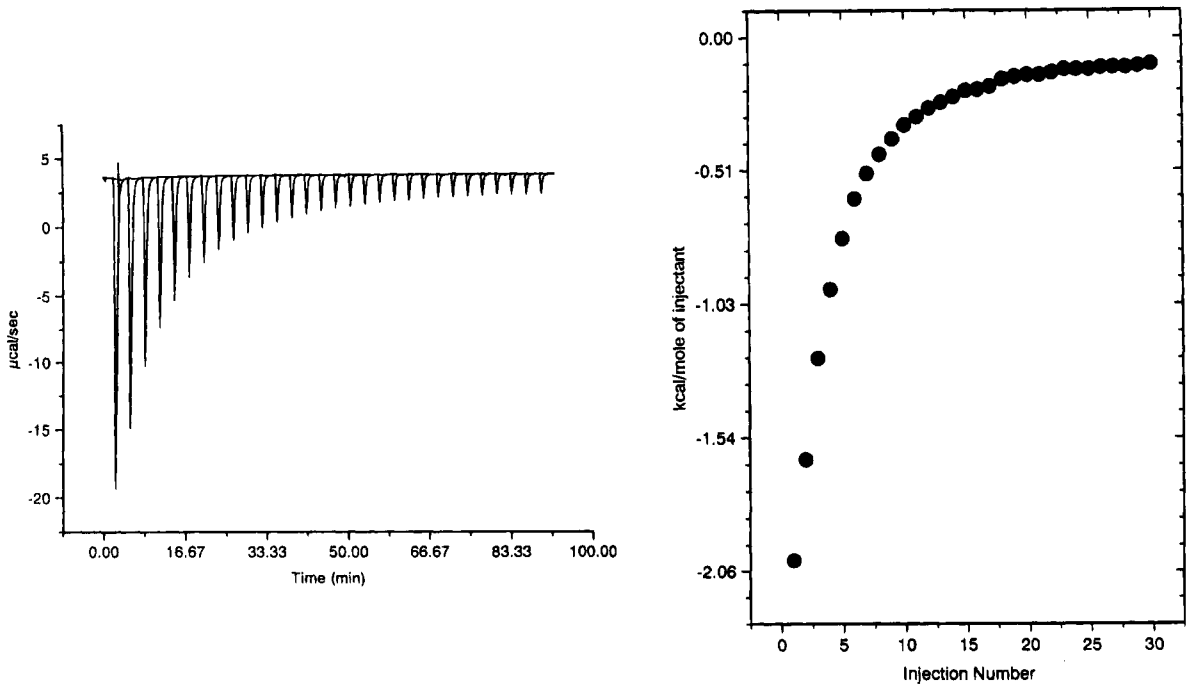

FIGURE 2: Raw (left) and integrated (right) calorimetric data for binding of the P^k trisaccharide to the SLT-1 B-subunit. Titration was in 10 mM MOPS buffer (pH 7.38), 138 mM NaCl, and 10 mM KCl at 10 °C. B-subunit monomer concentration: 0.3635 mM. Carbohydrate (55 mM) was injected in 7 μL aliquots.

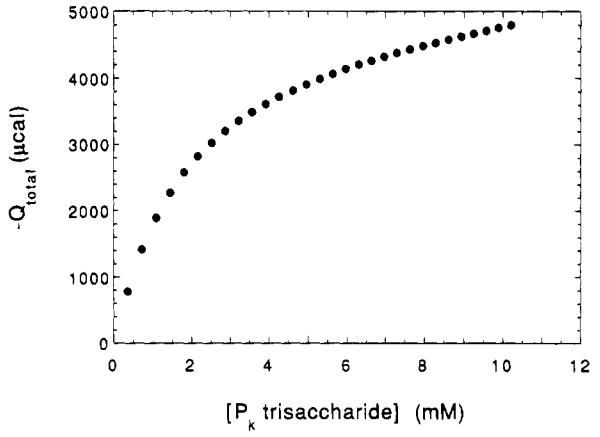

FIGURE 3: Integrated enthalpy of binding as a function of the P^k trisaccharide concentration. Conditions are as for Figure 2.

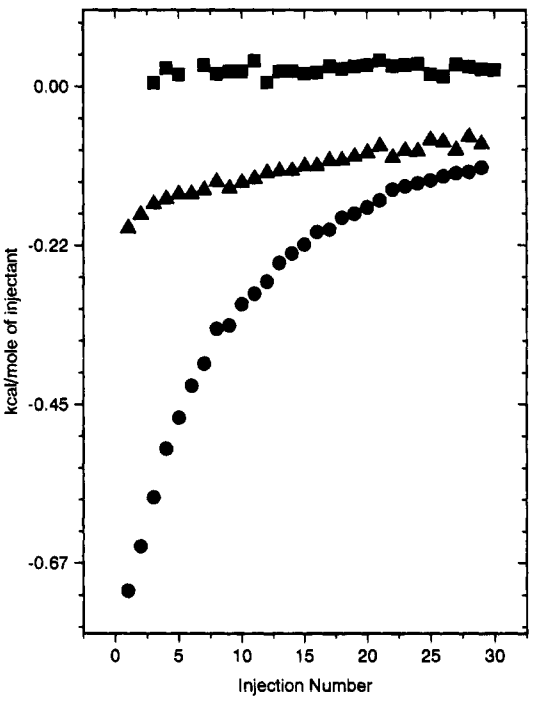

FIGURE 4: Integrated binding data for SLT-1 B-subunit with β-methyl lactoside (■), β-methyl galabioside (▲), and P^k trisaccharide (●). In all cases, reactions were run in 10 mM MOPS (pH 7.38), with 138 mM NaCl and 10 mM KCl at 30 °C. B-subunit monomer concentrations in each case were 0.312 mM. P^k trisaccharide (55 mM) was injected in 7 μL aliquots, β-methyl galabioside (60 mM) in 8 μL aliquots, and β-methyl lactoside (60 mM) in 8 μL aliquots.

of other lectin−carbohydrate interactions that have been evaluated calorimetrically (Schwarz et al., 1991; Sigurskjold et al., 1991; Williams et al., 1992; Toone, 1994). Measurements of ΔH over a temperature range of 30 °C yielded a ΔC_p of −40 eu, again in good agreement with the values of other lectin−carbohydrate interactions (Figure 5). On the basis of a limited set of reported calorimetric studies of protein−carbohydrate interactions, we have previously noted that heat capacity changes during lectin−carbohydrate binding are substantially different from those for antibody−carbohydrate binding (Williams et al., 1992). While the data set remains too small to reach unambiguous conclusions, these differences may signal alternative molecular mechanisms of protein−carbohydrate association in lectin vs antibody recognition. In contrast to other protein−carbohydrate interactions, the enthalpy−entropy compensation for SLT-1 oligosaccharide binding as a function of temperature is not perfect, and binding constants vary by a factor of 2 over the temperature range studied, falling with increasing temperature (Figure 5). The implications of this phenomenon in cell binding assays, where measurements at different temperatures are used to differentiate binding and metabolic processes, have been discussed (Schön & Freire, 1989).

The isolated B-subunit shows a distinct asymmetry in the deposited crystal structure (Hart et al., 1991; Stein et al., 1992). While the asymmetry is not present in the structure of the holotoxin, we were concerned nontheless with both the stoichiometry of binding and issues of cooperativity. We

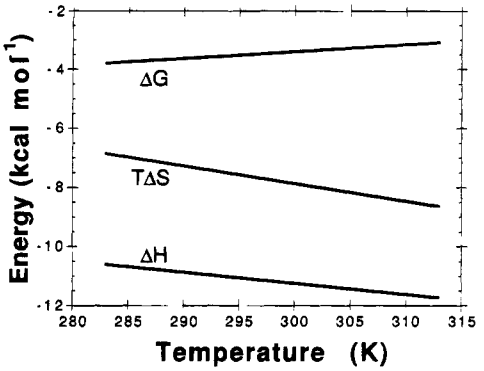

FIGURE 5: Gibbs free energy, enthalpy, and entropy of interaction of the P^k trisaccharide with the SLT-1 B-subunit as a function of temperature.

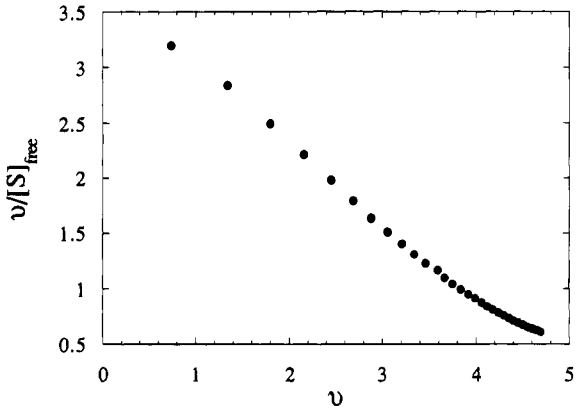

FIGURE 6: Scatchard analysis of SLT-1 B-subunit P^k trisaccharide binding. Conditions are as for Figure 2.

therefore created Scatchard plots from binding data as outlined in the Materials and Methods section (Figure 6). The plots clearly indicate five binding sites per B-subunit pentamer. The issue of cooperativity and/or identical sites is somewhat less definitive. The plots are slightly concave up, generally an indication of either multiple classes of sites or negative cooperativity. Alternatively, the lack of any sigmoidal deviation from the expected hyperbolic shape in Figure 3 supports identical, non-interacting sites. The shape of Scatchard plots generated from calorimetric data is sensitive to the value of ΔH used in eq 4. In systems where binding constants are large, it is possible to evaluate ΔH directly by making injections small enough that all of the ligand added is bound. For the weak bindings observed here, however, the only realistic source of ΔH is from the curve fit to eq 2. Thus, although on the basis of Figure 6 we cannot definitively categorize the binding sites of the B-subunit pentamer as identical and non-interacting, we are reluctant to interpret the relatively minor curvature in Scatchard plots.

A variety of solid-phase and biological binding assays examining the binding of the holotoxin/B-subunit to carbohydrate have been carried out (Fuchs et al., 1986; Lindberg et al., 1986; Lingwood et al., 1987; Jacewicz et al., 1989; Brown et al., 1991). These assays typically measure the affinity of the toxin for HeLa or Vero cells or for isolated glycolipids containing the αGal(1→4)Gal linkage. Frequently, a slow binding phenomenon is observed, and in some experiments several hours are required for the system to reach equilibrium. The unique advantage of calorimetric evaluation of protein−carbohydrate association is that soluble, monomeric saccharide interacts with soluble receptor, and the resulting thermicities reflect only protein−carbohydrate

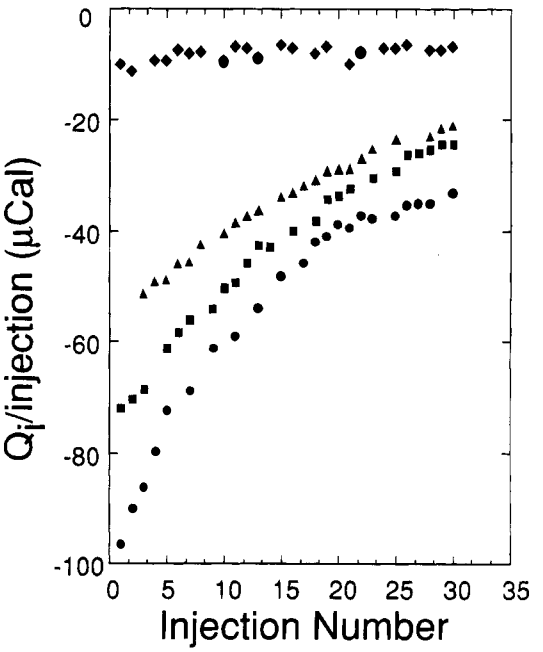

FIGURE 7: SLT-1 B-subunit interactions at pH 7.38 (MOPS, ●), 6.05 (3,3-dimethylglutarate, ■), 5.03 (3,3-dimethylglutarate, ▲), and 4.01 (3,3-dimethylglutarate, ◆). In all cases, titrations were run at 30 °C and the buffers were augmented with 138 mM NaCl and 10 mM KCl. B-subunit monomer concentrations were 0.16, 0.17, 0.16, and 0.17 mM, respectively. In all cases, the P^k trisaccharide concentration was 55 mM and 3.2 μL injections were used.

interactions. In titrations of various saccharides with the B-subunit, we see no evidence of any process with a time constant longer than that of the calorimeter (~10 s^{-1}), even at temperatures as low as 10 °C. The slow binding observations in heterogeneous solid-phase or biological assays are likely a result of some phenomenon other than protein−carbohydrate complexation. Our observations again point to the danger of interpreting complex, competitive binding bioassays solely in terms of the protein−carbohydrate interaction.

The role of endosomal pH has been discussed via-à-vis the mechanism of entry of the A-subunit into the cytosol (Saleh & Gariepy, 1993). We investigated the binding of SLT-1 B-subunit to the P^k trisaccharide as a function of pH from 7.2 to 4.0 (Figure 7). The binding is strongly a function of pH: binding is substantially impaired at pH 6.0 and essentially nonexistent below pH 5.0. This is consistent with the suggestion that a group of aspartate carboxylates is involved in saccharide binding (Jackson et al., 1990). The implications of impaired carbohydrate binding at endosomal pH are unclear, since the role of the B-subunit in toxin entry remains elusive. We note, however, that if the B-subunit facilitates the entry of the A-subunit into the cytosol following endocytosis, protein−carbohydrate interaction cannot be invoked as a mechanism for toxin−membrane adhesion during vesicle acidification.

In some titrations of the SLT-1 B-subunit with either the P^k trisaccharide (Figure 8) or β-methyl galabioside, a significant baseline break was observed. The break occurred only under certain conditions, notably in phosphate buffer. The position of the break was dependent on both the total carbohydrate concentration and the size of the aliquot added (Figure 8). Substantially more β-methyl galabioside than P^k trisaccharide was required to induce baseline deflection (data not shown). The break was not observed in titrations

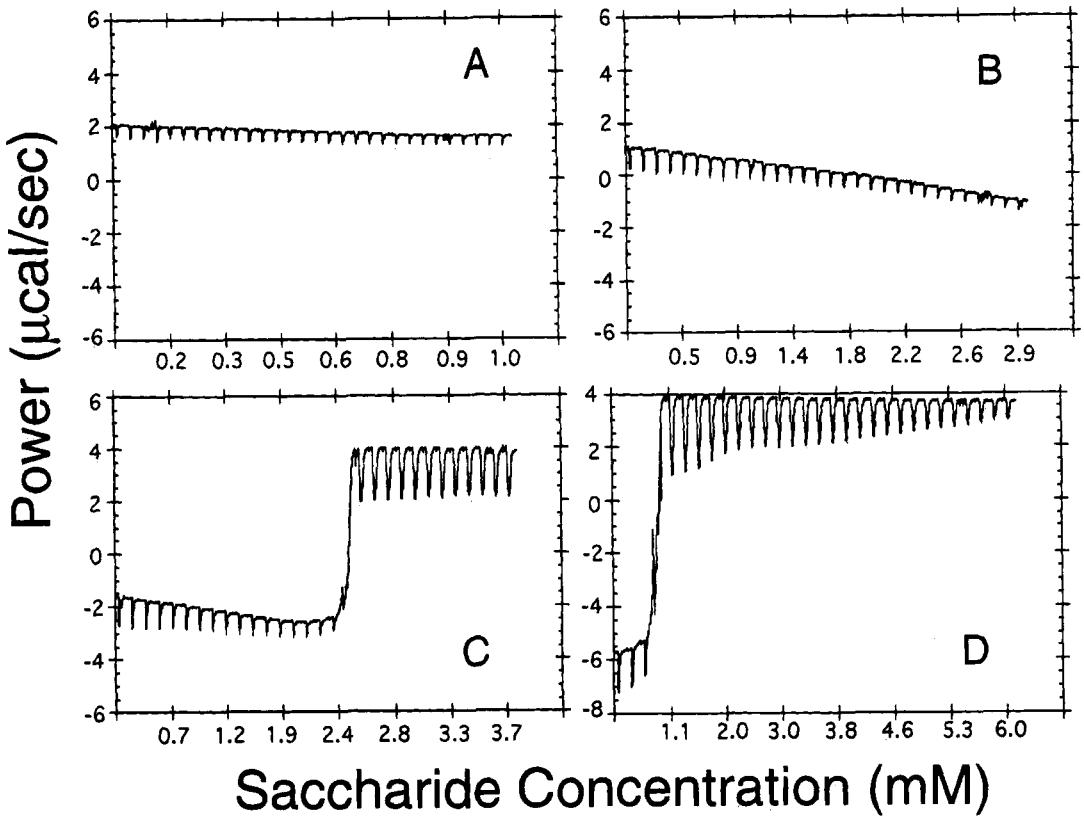

FIGURE 8: SLT-1 B-subunit−P^k trisaccharide binding in 10 mM phosphate buffer at 30 °C: (A) 20 mM trisaccharide, 2.5 μL injections; (B) 30 mM trisaccharide, 4.9 μL injections; (C) 30 mM trisaccharide, 6.5 μL injections; (D) 35 mM trisaccharide, 8 μL injections. In all cases, titrations were run at pH 7.28 in 138 mM NaCl and 10 mM KCl; the B-subunit monomer concentration was 0.12 mM throughout.

with β-methyl lactoside or methyl β-galactopyranoside at any carbohydrate concentration or aliquot size. The break is highly cooperative, and we were unable to create multiple breaks of smaller increments, regardless of the size of the carbohydrate aliquot added. Two control experiments unambiguously demonstrate that the break is the result of protein−carbohydrate interaction. Competent B-subunit titrated with methyl α-mannopyranoside, which does not interact with the toxin binding subunit, produced no break at any carbohydrate concentration. Similarly, a B-subunit mutant (Phe30Ala) known to have a 15-fold-reduced carbohydrate binding constant was titrated with P^k trisaccharide; at no time was a baseline break observed (Clark et al., unpublished experiments).

The calorimeter used for these experiments is a continuous power compensation design, and the ordinate records the difference in power required to keep the reference and sample cells at identical temperatures. A break in the baseline therefore represents a change in the effective heat capacity of the cell. For the experiments here, the calorimeter cell is heated at a rate of 110 μcal s^{-1}: a change in baseline position of 6 μcal s^{-1} thus represents a change in the heat capacity of ~5%. This change is too large to be accounted for reasonably by a change in the heat capacity of the protein as a result of binding; under the experimental conditions, protein accounts for <0.1% of the total mass of the cell. We therefore suspected that aggregation or precipitation of the protein, resulting in altered thermal conductivity patterns in the cell, might be the cause of the baseline shift.

To probe the validity of our aggregation hypothesis, we carried out a protein−carbohydrate titration monitoring average particle size as a function of carbohydrate concentration by dynamic light scattering. The results of these experiments (Figure 9) clearly indicate an increase in average particle size as the carbohydrate concentration increases. Furthermore, the distribution of particle sizes broadens with increasing carbohydrate concentration, as would be expected for an aggregation process. However, the average particle size increases in a monotonic, steady pattern, and no sudden increase in particle size was observed, in contrast to calorimetric titrations. The protein concentrations in the two experiments were similar (0.12 mM for the calorimetry vs 0.071 mM), and the concentrations of carbohydrate resulting in increased particle size in light scattering experiments were similar to the minimum concentrations causing baseline breaks in calorimetric titrations (1.1 mM for calorimetry vs 1.5 mM for light scattering). The reason for a single baseline break in calorimetric titrations is not completely understood at this point, although it likely represents a higher order effect, such as the precipitation of protein on the cell walls or aggregation of oligomers into higher order structures.

We attribute the aggregation of the protein to hydrophobic interactions. Support for a hydrophobic aggregation is provided by the suppression of aggregation during SLT-1−oligosaccharide binding by the choice of buffer. The use of MOPS buffer, instead of PBS, provided normal calorimetric traces with no baseline breaks. It is well known that neutral salts enhance or diminish hydrophobic interactions in solution and that phosphate stabilizes protein structure in many cases because of its enhancement of hydrophobic effects (von Hippel & Wong, 1964). MOPS buffer is not predicted to enhance hydrophobic effects; hence, a suppression of aggregation is observed.

Aggregation of other bacterial two-component toxins in solution has been observed. The diphtheria toxin aggregates both in reponse to low pH and during association with

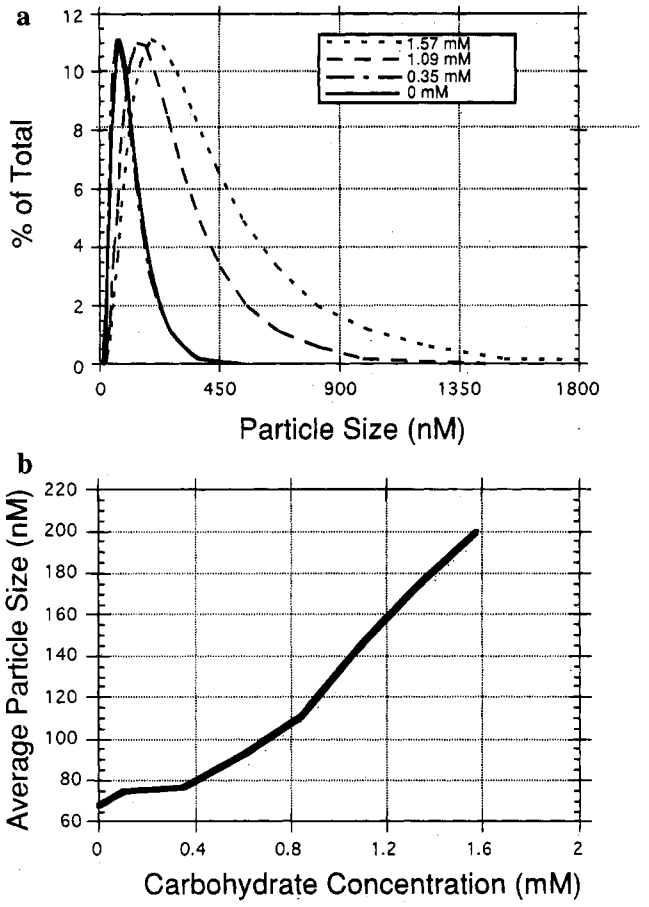

FIGURE 9: SLT-1 B-subunit dynamic light scattering as a function of P^k trisaccharide concentration. B-subunit pentamer concentration: 0.071 mM in 10 mM phosphate buffer (pH 7.28), 138 mM NaCl, and 10 mM KCl. (a) Particle size distribution at 0.00, 0.35, 1.09, and 1.57 mM trisaccharide. (b) Average particle size as a function of P^k trisaccharide.

membranes (London, 1992b), and cholera toxin bound to G_{M1}-containing liposomes aggregates into two-dimensional crystals (Ribi et al., 1988). Aggregation of the diphtheria toxin at low pH is attributed to contact between hydrophobic sites unmasked either by protein reorganization or by protonation of charged acidic side chains (London, 1992a). More recently, Spangler and co-workers also observed that binding of the pertussis toxin, also of the AB_5 structure, to inert polypropylene surfaces was enhanced by the addition of soluble glycoprotein or oligosaccharide receptor analogs (Spangler et al., 1993). The enhanced binding was attributed to the exposure of hydrophobic residues upon saccharide binding. Although the investigators did not comment on the aggregation state of the protein, it follows that in aqueous solution exposure of hydrophobic surfaces would lead to aggregation.

We conclude that SLT-1 B-subunit carbohydrate binding is accompanied by aggregation and that this aggregation is responsible for the baseline break observed in the calorimetric titrations.

Optical Spectroscopy. The results of calorimetry and light scattering studies indicate that a hydrophobic aggregation process accompanies SLT-1 B-subunit−saccharide binding. These hydrophobic interactions may arise either from structural reorganization of the B-subunit during binding that exposes a hydrophobic site or from masking of a charged hydrophilic patch of the protein by carbohydrate. To elucidate the molecular origin of aggregation, we turned to optical spectroscopy as a probe of native structure during binding.

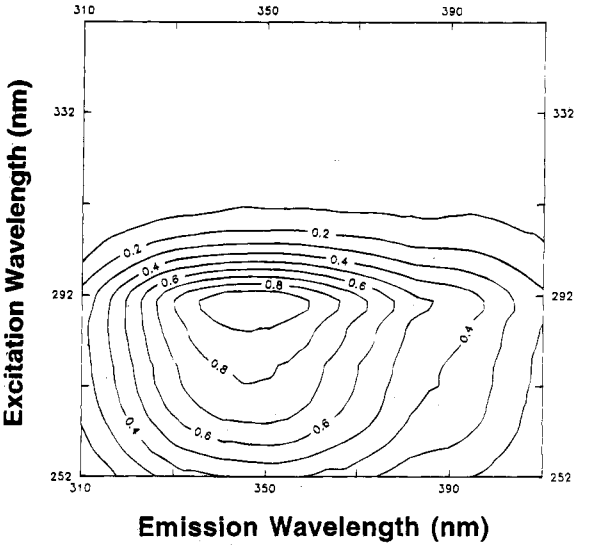

FIGURE 10: Excitation−emission matrix of SLT-1 B-subunit. B-subunit (0.107 mM) was in 10 mM phosphate buffer (pH 7.28), 138 mM NaCl, and 10 mM KCl.

We first examined the fluorescence spectra of native and F30A mutant B-subunits in the free and bound forms. Each B-subunit contains one tryptophan, two tyrosines, and four phenylalanines: each of these residues could, in principle, contribute to the fluorescence of the protein. To evaluate the contributions of tyrosine and phenylalanine to total protein fluorescence, we obtained an excitation−emission matrix exciting at 250−310 nm (Figure 10). The matrix indicated a single fluorescence maximum, with identical emission bands resulting from excitation at either 275 or 295 nm. These observations define tryptophan as the sole source of SLT-1 B-subunit fluorescence (Konev, 1967). The emission maximum at 346 nm (Figure 10), intermediate between type II and III spectra, is consistent with a largely solvent-exposed indole (Permyakov, 1993). This observation is consistent with crystallographic studies of the B-subunit that show the tryptophan indole ring at the bottom of the α-helical segment (i.e., distal to the A-subunit) and directed toward the central pore of the B-subunit pentamer (Stein et al., 1992). The tryptophan shows a characteristic biexponential decay (Table 1), which is indicative of a rotomeric population distribution of the indole ring.

The fluorescence of the SLT B-subunit was evaluated in the bound form under several conditions. In each case, enough carbohydrate was added to result in >90% bound B-subunit (30 mM). When P^k trisaccharide was added in a single aliquot to protein in PBS, the total fluorescence intensity approximately doubled (Table 1). A 4-fold increase in the intensity of the peak at 295 nm, assigned to physical scattering, was also observed. These observations clearly are consistent with the aggregation phenomenon discussed earlier. The longer lifetime shifted following carbohydrate addition (Table 1), and the fractional contribution of the long and short lifetimes to overall relaxation also changed. Although both prior to and following saccharide addition the emission maxima are broad, there appears to be a change in the position of the emission maximum from 346 to 354 nm, which is indicative of a change in solvent exposure during binding. To examine the effect of the mode of carbohydrate addition, an identical experiment was per-

Table 1: F30A Mutant and Native B-Subunit Fluorescence When Free in Solution or Bound to P^k Trisaccharide[a]

	free				bound			
	lifetime (ns)	fraction (%)	EM max (nm)	intensity (abs units)	lifetime (ns)	fraction (%)	EM max (nm)	intensity (abs units)
native SLT-1	1.3	72	347	419	1.1	55	354	815
in PBS	6.9	28			7.8	45		
F30A mutant	1.3	66	349	357	1.3	52	344	402
in PBS	6.3	34			6.2	48		
native SLT-1	1.0	55	333	466	1.2	47	337	521
in MOPS[b]	6.6	45			6.9	53		

[a] Conditions are the same as for Figure 11. [b] MOPS buffer was 10 mM (pH 7.38), supplemented with 138 mM NaCl and 10 mM KCl.

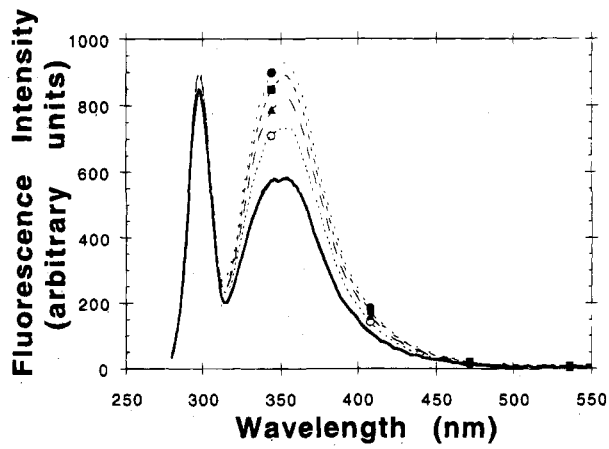

FIGURE 11: SLT-1 B-subunit fluorescence as a function of P^k trisaccharide. B-subunit: 0.107 mM (2.9 mL) in PBS, pH 7.38. P^k trisaccharide in PBS was added in four 25 μL increments to a final concentration of 30 mM. Symbols: 0 mM (—); 6.91 mM (○); 13.63 mM (▲); 20.42 mM (■); 27.0 mM (●).

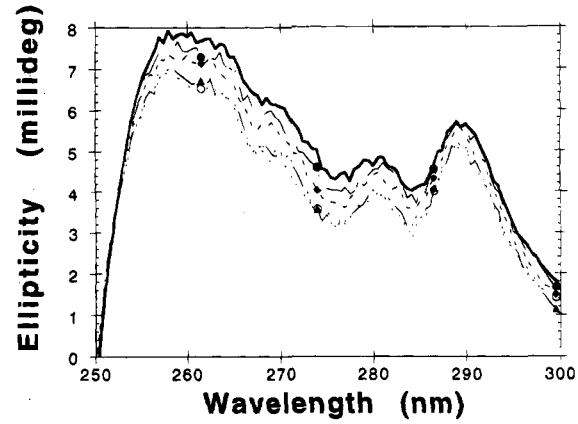

FIGURE 12: Near-UV CD spectra of native B-subunit as a function of P^k trisaccharide. Protein (0.253 mM, 2.5 mL) was in PBS, pH 7.38. P^k trisaccharide in PBS (pH 7.38) (206 mM) was added in 20 μL increments: 0 mM (—); 4.12 mM (●); 8.24 mM (◆); 12.36 mM (▲); 20.60 mM (○).

formed, except that carbohydrate was added in four equal aliquots. An increase in fluorescence intensity similar to that accompanying single aliquot addition was observed (Figure 11), although the alterations in fluorescence lifetimes were not as pronounced. Physical light scattering also increased, but much less dramatically than it did in the single aliquot experiment. Likewise, there was a slight shift in the position of the emission maximum from 346 to 353 nm.

To rule out nonspecific origins for the altered tryptophan spectra, we added 30 mM P^k trisaccharide to F30A SLT B-subunit in PBS. At 30 mM carbohydrate, an increase in the fluorescence of ~10% was observed (Table 1). This increase is in reasonable agreement with the fraction of B-subunit predicted to be bound at 30 mM P^k trisaccharide (5−6%), assuming similar photophysical behavior for the fully bound proteins. There was also very little change in the fluorescence lifetimes or in the position of the emission maximum compared to the case of the native B-subunit (Table 1).

The fluorescence spectroscopic studies clearly indicate a change in tryptophan orientation following binding, as well as significant protein aggregation. To investigate a possible link between tryptophan reorientation and protein aggregation, we carried out a similar experiment in MOPS buffer, which we have previously shown to suppress aggregation. In MOPS, the fluorescence emission maximum is blue shifted relative to PBS, showing a maximum near 333 nm. The addition of carbohydrate in a single aliquot resulted in an approximately 10% increase in total fluorescence intensity (Table 1) and a slight increase in the physical light scattering. There was, however, no change in the fluorescence lifetimes.

These data suggest that a shift in the indole conformational equilibrium, as measured by changes in fluorescence spectra, correlates with protein aggregation. Clearly, it is impossible to differentiate the case in which binding alters the tryptophan orientation, which then induces aggregation, from a scenario in which carbohydrate binding induces aggregation in some other way, which in turn alters the tryptophan environment. In any event, these studies establish a plausible molecular mechanism for the apparent hydrophobic aggregation that accompanies binding.

To further probe the nature of structural perturbations associated with carbohydrate binding, we examined CD spectra of native and F30A mutant B-subunits in free and bound forms. The CD spectra of the free B-subunits were characteristic of proteins whose structures are dominated by β-pleated sheets. The near-UV CD spectrum shows three maxima near 260, 280, and 290 nm. Both the near- and far-UV CD spectra of the F30A mutant and native proteins were identical, indicating that a single amino acid substitution in the putative binding site (Phe30 to Ala30) does not perturb the secondary structure of the B-subunit. This observation is consistent with X-ray crystallographic data obtained for the F30A mutant and the native B-subunits (Stein et al., 1992; Clark et al., unpublished experiments).

CD spectra were also recorded under conditions such that >90% of the protein would be bound (i.e., 30 mM trisaccharide). No change in the far-UV CD spectra of the native B-subunit was observed upon addition of P^k trisaccharide, suggesting that no significant reorganization of the B-subunit backbone structure takes place during carbohydrate binding. Alternatively, a decrease in ellipticity at all three maxima of the near-UV CD was observed, with the maximum difference of 20% occurring in the maximum near 260 nm (Figure 12). The change in signal titrates in a normal fashion with added saccharide, with the change approaching 50% of maximum near 5 mM, in good agreement with the

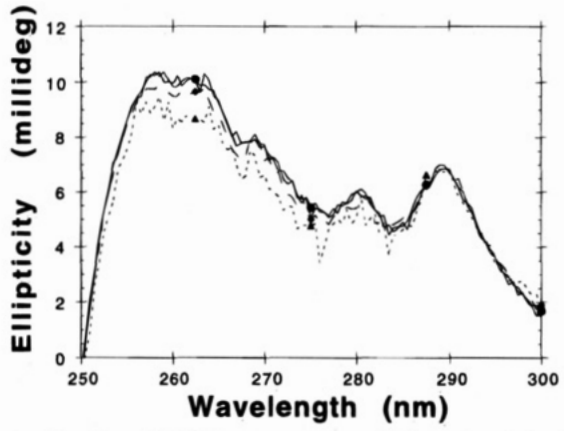

FIGURE 13: Near-UV CD spectra upon addition of carbohydrate for F30A mutant B-subunit. Protein (0.107 mM, 2.5 mL) was in PBS, pH 7.38. P^k trisaccharide in PBS (pH 7.38) (270 mM) was added in 20 μL increments: 0 mM (—); 5.4 mM (●); 16.2 mM (◆); 27.0 mM (▲).

dissociation constant of 1−2 mM derived from titration microcalorimetry. Titration of the P^k trisaccharide into mutant B-subunit also resulted in a decrease in ellipticity in the near-UV CD spectra centered maximally near 260 nm. However, the difference was slightly less than that for the native B-subunit (15%) (Figure 13), and there was no decrease in the ellipticity near 290 nm. Near-UV CD difference spectra arise from perturbations of aromatic amino acid side chains, with the wavelength of maximal difference closely correlating to the simple absorbance maximum of the chromophore (Woody, 1994). Therefore, the changes in the near-UV CD maximum near 260 nm could result from perturbations of either a tyrosine, a phenylalanine, or both, while the UV signal at 290 nm likely is due solely to tryptophan. Each monomer of the B-subunit pentamer contains a single tryptophan (position 34), two tyrosines (positions 11 and 14), and four phenylalanines (positions 20, 30, 63, and 68) (Seidah et al., 1986). The lack of a decrease in ellipticity at 290 nm for the F30A mutant B-subunit is consistent with its much reduced binding from microcalorimetric studies.

From the optical spectroscopic data, it is clear that binding of the P^k trisaccharide to the SLT-1 B-subunit perturbs the environment of the tryptophans in the central helical core. Crystal structures of the SLT-1 B-subunit and the holotoxin reveal that tryptophan 34 can exist in at least two different rotomeric orientations. In the first orientation, the indole ring is angled toward the central pore of the pentamer, away from solvent (Figure 14a). In the second orientation observed in the holotoxin, it is angled downward, away from the central pore and toward bulk solvent (Figure 14b). *We propose that carbohydrate binding perturbs the rotomeric equilibrium in favor of the orientation in which the indole ring is solvent exposed. This shift in conformation renders the protein more hydrophobic and leads to aggregation in vitro.*

The mechanism by which this shift in rotomeric equilibrium occurs is unclear. One possibility is that interaction of the terminal galactose ring of the P^k trisaccharide with

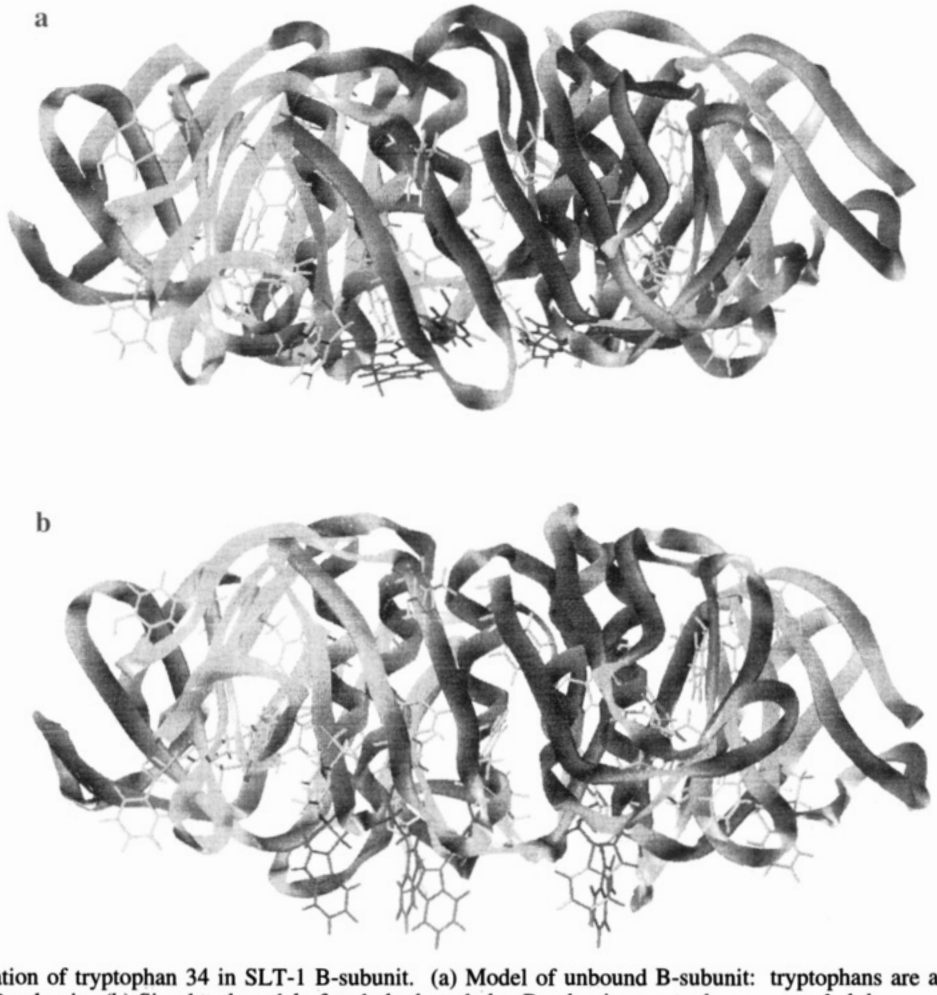

FIGURE 14: Orientation of tryptophan 34 in SLT-1 B-subunit. (a) Model of unbound B-subunit: tryptophans are angled up toward the central pore of the B-subunit. (b) Simulated model of carbohydrate-laden B-subunit: tryptophans are angled down, away from the central pore and toward bulk solvent.

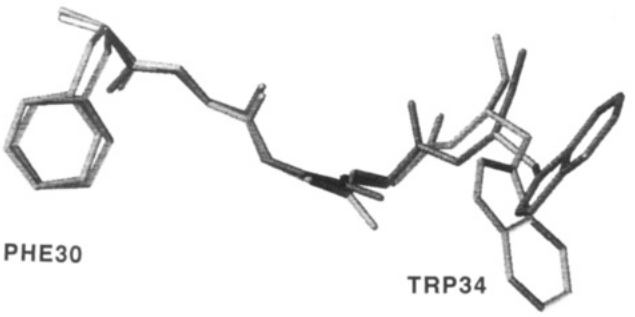

FIGURE 15: Superimposition of models of the B-subunit with tryptophan in two different orientations. Only residues 30−34 are shown.

phenylalanine 30, known to be required for binding, induces a change in the tryptophan orientation by reorienting the Cα backbone. This mechanism seems unlikely on the basis of crystallographic data. Figure 15 shows residues 30−34 of the B-subunit superimposed with the tryptophans in the up and down orientations. There is no significant change in the Cα backbone between the two orientations. Thus, at a minimum, both conformers are possible without backbone reorganization. Alternatively, the rotomeric equilibrium could be perturbed by direct contact of the P^k trisaccharide with the central tryptophan. The distance between the indole ring and phenylalanine 30, presumably part of the binding site, is 11.4 Å with the indole ring in the down position, making direct carbohydrate−indole interaction feasible in only one of the two orientations.

Mechanism of Cell Entry. The mode of entry of the A-subunit of bacterial two-component toxins into the cytosol from the endosome remains unknown. Largely on the basis of work with structurally related toxins, two models have been proposed, differing in the role of the B-subunit. In the first, the B-subunit is proposed to assist the entry of the toxic component by forming a pore in the membrane, allowing the A-subunit entry into the cytosol. Several lines of evidence support this hypothesis. First, the *E. coli* heat-labile toxin, structurally similar to the SLT-1, binds with the A-subunit directed away from the cell membrane (Sixma et al., 1992). In the absence of assistance from the B-subunit, a mechanism for bringing the A-subunit into contact with the cell membrane is lacking. Second, no A-subunit examined to date contains the classical membrane-spanning hydrophobic α-helical segments that would presumably be necessary for unassisted transport of the A-subunit across the cell wall (London, 1992a). Third, cholera toxin B-subunits are capable of inducing ion channels in planar lipid bilayers, suggesting that the B-subunit may enter and span lipid bilayers (Krasilnikov et al., 1991). Furthermore, the outer portion of the SLT-1 B-subunit, like other members of the class, is composed of a series of hydrophobic β-sheets, reminiescent of other membrane-inserting proteins (Weiss et al., 1991). Numerous biophysical studies show that a substantial portion of the diphtheria toxin is buried in the lipid membrane during binding (London, 1992b). Finally, the width of the B-subunit is sufficient to span most

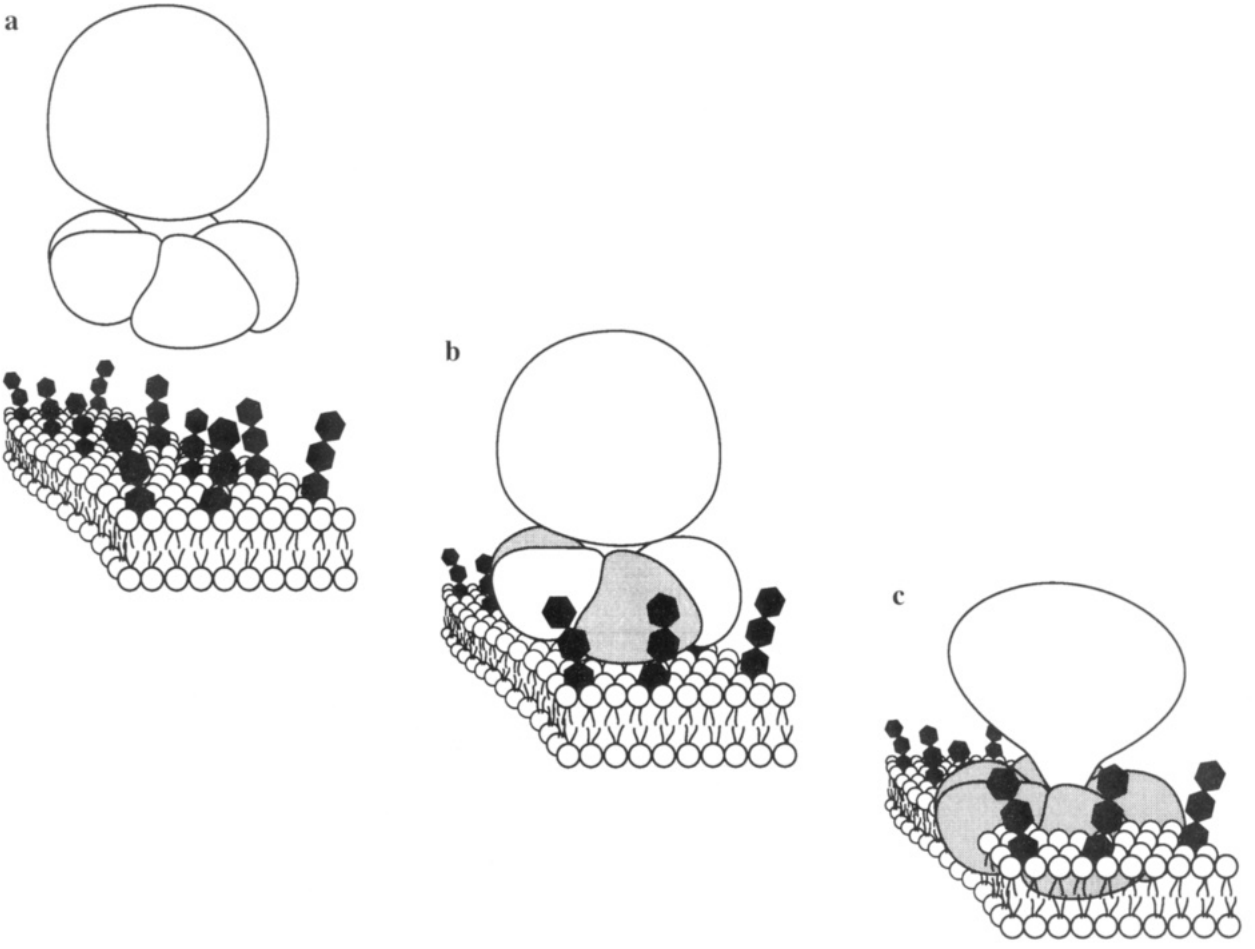

FIGURE 16: SLT-1 B-subunit cell-surface binding. (a) Intact holotoxin approaches the cell surface distal to the A-subunit and begins to bind with cell-surface glycolipids. (b) Carbohydrate binding results in either the exposure of hydrophobic surface area on the B-subunit or the masking of charged surface area. (c) B-subunit−lipid bilayer interaction draws the toxin into the endosomal membrane, where at lowered pH levels the A-subunit dissociates and is transported to the cytosol with assistance from the B-subunit.

membranes (London, 1992a). In an alternative proposal, the A-subunit passes through the membrane unassisted by the B-subunit. This proposal is based on experiments, including photolabeling, electron diffraction, and quasi-elastic light scattering, that suggest that the B-subunit of the cholera toxin does not significantly penetrate into the membrane following carbohydrate binding (Tomasi & Montecucco, 1981; Wisnieski & Bramhall, 1981; Dwyer & Bloomfield, 1982; Ribi et al., 1988). In no cases, however, were conditions that mimic those found at cells surfaces during endocytosis utilized.

We propose a mechanism of B-subunit adhesion that invokes both protein−carbohydrate and protein−lipid interactions. In this model, weak interaction of $GbOse_3$ with the pentamer perturbs the tryptophan 34 rotomeric equilibrium toward the extended, solvent-exposed form. The now hydrophobic B-subunit face forms new interactions with the lipid bilayer, tightly holding the toxin to the cell surface (Figure 16). Our experiments do not address the extent of penetration of the B-subunit into the membrane nor the mechanism of A-subunit transport across the endosomal membrane, but they clearly suggest that an interaction other than protein−carbohydrate, and most likely protein−lipid, is responsible for adhesion of the toxin to cell surfaces.

In addition to the considerable body of supporting literature data outlined here, our model is based on three observations from this work. First, it is clear that saccharide binding induces aggregation in comparatively concentrated (millimolar) solution, most likely in a process involving hydrophobic interactions. This hydrophobic aggregation provides a molecular mechanism for B-subunit−lipid bilayer adhesion. We note parenthetically that a large enthalpy of protein−carbohydrate interaction is not reflected in the free energy of binding; much of the binding enthalpy may be used to drive an entropically unfavorable conformational reorganization. That conformational reorganization is involved in binding is also reflected in a small ΔC_p. A heat capacity change of only 40 eu, coupled with an entropy of binding of 25 eu, suggests a large unfavorable ΔS_{config} (Murphy & Gill, 1991; Schön & Freire, 1989; Toone, 1994). Second, the A-subunit clearly must stay in contact with the endosomal membrane during transport to the cytosol, regardless of the involvement of the B-subunit in the process. Our results indicate that protein−carbohydrate interaction cannot support the adhesion of holotoxin to the membrane at endosomal pH. Finally, we note that the binding constants of both Shiga and cholera toxin binding to intact cells are similar ($\sim 10^9$ M^{-1}), *despite a 10^3 difference in per site carbohydrate binding affinities* (Cuatrecasas, 1973; Holmgren et al., 1974). This similarity suggests a common mechanism of adhesion that does not involve protein−carbohydrate interaction.

Although it is clear that protein−carbohydrate interaction controls a myriad of biological events, the chronically low binding constants for protein−carbohydrate couples raise significant questions regarding the precise roles of carbohydrates in biological communication. The model proposed here is reminiscent of other carbohydrate-based biological recognition systems: *protein−carbohydrate interaction is involved in specificity, but not tight binding*. This principle has been best demonstrated for neutrophil recruitment, where recognition is mediated by protein (ELAM)−carbohydrate (sialyl Le^x) binding, but tight binding and flattening are the result of protein−protein binding (Mulligan et al., 1993). The generality of the motif awaits detailed structural and energetic studies of a much larger group of carbohydrate-mediated biological recognition systems.

ACKNOWLEDGMENT

We thank Professor J. Brunton for the generous gift of the B-subunit-expressing strain and for many helpful discussions. We also thank Dr. G. Whitesell of Glaxo Inc. for assistance in collecting light scattering data, Scott Lee for collecting the excitation−emission matrix, and Bradley Isbister for protein modeling.

SUPPLEMENTARY MATERIAL AVAILABLE

Details of the syntheses of P^k trisaccharide, β-methyl lactoside, and β-methylgalabiose (12 pages). Ordering information is given on any current masthead page.

REFERENCES

Bevington, P. R. (1969) *Data Reduction and Error Analysis for the Physical Sciences*, p 235, McGraw-Hill, New York.

Boyd, B., & Lingwood, C. (1989) *Nephron 5*, 207−210.

Brown, J. E., Ussery, M. A., Leppla, S. H., & Rotham, S. W. (1980) *FEBS Lett. 117*, 84−88.

Brown, J. E., Echeverria, P., & Lindberg, A. (1991) *Rev. Infect. Dis. 13* (Suppl. 4), S298−303.

Centers for Disease Control and Prevention Leads from the Morbidity and Mortality Weekly Report, Atlanta, GA (1993) *J. Am. Med. Assoc. 269* (10), 2194−96.

Cimolai, N., Carter, J. E., Morrison, B. J., & Anderson, J. D. (1990) *J. Pediatr. 116*, 589−592.

Clark, C., Bast, D., Sharp, A., St. Hilaire, P., Agha, R., Stein, P., Toone, E., Read, R., & Brunton, J. (1994) *J. Cell Biol.* (submitted for publication).

Cox, D. D., Metzner, E., & Reist, J. E. (1978) *Carbohydr. Res. 63*, 139−47.

Cuatrecasas, P. (1973) *Biochemistry 12*, 3547−58.

Donohue-Rolfe, A., Jacewicz, M., & Keusch, G. T. (1989) *Mol. Microbiol. 3*, 1231−36.

Dubois, M., Giles, K. A., Hamilton, J. K., Rebers, P. A., & Smith, F. (1956) *Anal. Chem. 28* (3), 350−356.

Dwyer, J. D., & Bloomfield, V. A. (1982) *Biochemistry 21*, 3227−31.

Edelhoch, H. (1967) *Biochemistry 6* (7), 1948−54.

Fraser, M., Chernaia, M., Kozlov, Y., & James, M. N. (1994) *Nature Struct. Biol. 1* (1), 59−64.

Fuchs, G., Mobassaleh, M., Donohue-Rolfe, A., Montgomery, R., Gerard, R., & Keusch, G. (1986) *Infect. Immun. 53* (2), 372−378.

Garegg, P. J., & Oscarson, S. (1985) *Carbohydr. Res. 137*, 270−75.

Griffin, P. M., & Tauxe, R. V. (1991) *Epidemiol. Rev. 13*, 60−98.

Griffin, P. M., Ostroff, S. M., Tauxe, R. U., Greene, K. D., Wells, J. G., Lewis, J. H., & Blake, P. A. (1988) *Ann. Intern. Med. 109*, 705−12.

Hart, P. J., Monzingo, A., Donohue-Rolfe, A., Keusch, G., Calderwood, S., & Robertus, J. (1991) *J. Mol. Biol. 218*, 691−694.

Holmgren, J., Mansson, J.-E., & Svennerholm, L. (1974) *Med. Biol. (Helsinki) 52*, 229−233.

Institute of Medicine Report (1992) *Emerging Infections: Microbial Threats to Health in the United States* (Shope, R., Lederberg, J., & Oakes, S., Eds.) National Academy Press, Washington, D.C.

Jacewicz, M., Feldman, H., Donohue-Rolfe, A., Balasubramanian, K., & Keusch, G. (1989) *J. Infect. Dis. 159*, 881−889.

Jackson, M., Waldolkowski, E., Weinstein, D., Holmes, R., & O'Brien, A. (1990) *J. Bacteriol. 172*, 653−658.
Keusch, G. T., Donohue-Rolfe, A., & Jacewicz, M. (1986) in *Microbial Lectins and Agglutinins Properties and Biological Activity*, p 271−295, John Wiley and Sons, New York.
Konev, S. (1967) *Fluorescence and Phosphorescence of Proteins and Nucleic Acids*, pp 69−78, Plenum Press, New York.
Krasilnikov, O. V., Muratkhodjaer, J. N., Voronov, A. T., & Yezepchuyk, V. Y. (1991) *Biochim. Biophys. Acta 1067*, 166−70.
Lee, L. A., Shapira, C. N., Hargrett-Bean, N., & Tauxe, R. V. (1991) *J. Infect. Dis. 164*, 894−900.
Lindberg, A. A., Schultz, J., Westling-Ryd, M., Brown, J. E., Rothman, S. W., Karlsson, K., & Stromberg, N. (1986) *Protein-Carbohydrate Interactions in Biological Systems*, pp 439−446, Academic Press, London.
Lindberg, A., Brown, E., Stromberg, N., Westling-Ryd, M., Schlutz, J., & Karlsson, K. (1987) *J. Biol. Chem. 262* (4), 1779−85.
Lingwood, C. A., Law, H., Richardson, S., Petric, M., Brunton, J., DeGrandis, S., & Karmali, M. (1987) *J. Biol. Chem. 262* (18), 8834−39.
London, E. (1992a) *Mol. Microbiol. 6* (22), 3277−82.
London, E. (1992b) *Biochim. Biophys. Acta 1113*, 25−51.
Mulligan, M. S., Paulson, J. C., Frees, S. D., Zheng, Z.-L., Lowe, J. B., & Ward, P. A. (1993) *Nature 364*, 149.
Murphy, P., & Gill, S. (1991) *J. Mol. Biol. 222*, 699−709.
O'Brien, A. D., & Tesh, V. L. (1991) *Mol. Microbiol. 5* (8), 1817−22.
Ostroff, S. M., Kobayashi, J. M., & Lewis, J. H. (1989) *J. Am. Med. Assoc. 262*, 355−359.
Permyakov, E. (1993) *Luminescence Spectroscopy of Proteins*, pp 57−77, CRC Press, Boca Raton, FL.
Ramotar, K., Boyd, B., Tyrrell, G., Gariepy, J., Lingwood, C., & Brunton, J. (1990) *Biochem. J. 272*, 805−811.
Reisbig, R., Olsnes, S., & Eiklid, K. (1981) *J. Biol. Chem. 256*, 8739−8744.
Ribi, H., Ludwig, D., Mercer, L., Schoolnik, G., & Kornberg, R. (1988) *Science 239*, 1272−39.
Rhode, J. E. (1984) *Rev. Infect. Dis. 6*, 840−54.
Saleh, M. T., & Gariépy, J. (1993) *Biochemistry 32*, 918−922.
Sandvig, K., Olsnes, S., Brown, J. E., Petersen, O., & van Deurs, B. (1989) *J. Cell. Biol. 108*, 1331−43.
Sandvig, K., Prydz, K., Ryd, M., & van Deurs, B. (1991) *J. Cell. Biol. 113*, 553−562.
Sandvig, K., Dubina, E., Garred Ø., Prydz, K., Kozlov, J., Hansen, S., & van Deurs, B. (1992) *Biochem. Soc. Trans. 20*, 724−727.
Schön, A., & Freire, E. (1989) *Biochemistry 28* (12), 5019−24.
Schwarz, F. P., Puri, K., & Surolia, A. (1991) *J. Biol. Chem. 266*, 24344−50.
Seidah, N., Donohue-Rolfe, A., Lazure, C., AuClair, F., Keusch, G., & Chrétien, M. (1986) *J. Biol. Chem. 261*, 13928−31.
Sigurskjold, B., Altman, E., & Bundle, D. (1991) *Eur. J. Biochem. 197*, 239−46.
Sixma, T. K., Pronk, S. E., Kald, K. H., van Zanten, B. A. M., Berghuis, A. M., & Hol, W. G. J. (1992) *Nature 355*, 561−64.
Spangler, B., Heerze, L., Clark, C., & Armstrong, G. (1993) *Arch. Biochem. Biophys. 305*, 153−158.
Stein, P. E., Boodhoo, A., Tyrrell, G. J., Brunton, J. L., & Read, J. R. (1992) *Nature 355*, 748.
Stoll, B. J., Glass, R. I., Hug, M. I., Khan, M. U., Bonu, H., & Holt, J. (1982) *J. Infect. Dis. 146*, 177−183.
Strockbine, N., Marques, L. R., Newland, J. W., Smith, H. W., Holmes, R. K., & O'Brien, A. D. (1986) *Infect. Immun. 53*, 735−40.
Strockbine, N., Jackson, M., Sung, L., Holmes, R., & O'Brien, A. (1988) *J. Bacteriol. 170* (3), 1116−1122.
Surewicz, W. K., Leddy, J. J., & Mantsch, H. M. (1990) *Biochemistry 29*, 8106.
Tomasi, M., & Montecucco, C. (1981) *J. Biol. Chem. 256*, 11177−81.
Toone, E. (1994) *Curr. Opin. Struct. Biol. 4*, 719−728.
von Hippel, P. H., & Wong, K.-Y. (1964) *Science 147*, 577−80.
Walterspiel, J. N., Ashkenazi, S., Morrow, A. L., & Cleary, T. G. (1992) *Infection 20* (1), 29−33.
Weiss, M. S., Abele, U., Weckesser, J., Welte, W., Schiltz, E., & Schulz, G. E. (1991) *Science 254*, 1627−30.
Williams, B., Chervenak, M., & Toone, E. (1992) *J. Biol. Chem. 267*, 22907−11.
Wiseman, T., Brandts, J., & Lin, L.-N. (1989) *Anal. Biochem. 179*, 131−137.
Wisnieski, B., & Bramhall, J. (1981) *Nature 289*, 319−321.
Woody, R. (1994) *Circular Dichroism Principles and Applications* (Nakanishi, K., Berova, N., & Woody, R., Eds.) VCH Publishers, Inc., New York.